Site- and rainfall-specific runoff coefficients and critical rainfall for mega-gully development in Kinshasa (DR Congo)

Jan Moeyersons, Fils Makanzu Imwangana & Olivier Dewitte

Natural Hazards
Journal of the International Society for the Prevention and Mitigation of Natural Hazards

ISSN 0921-030X

Nat Hazards
DOI 10.1007/s11069-015-1870-z

Springer

Nat Hazards
DOI 10.1007/s11069-015-1870-z

ORIGINAL PAPER

Site- and rainfall-specific runoff coefficients and critical rainfall for mega-gully development in Kinshasa (DR Congo)

Jan Moeyersons[1] · **Fils Makanzu Imwangana**[2,3] · **Olivier Dewitte**[1]

Received: 22 January 2015 / Accepted: 9 June 2015

Abstract This article presents a field-based method to assess site- and rainfall-specific runoff coefficients to be expected for a given period of the year. The method is applied to recognize soil uses/covers leading to reduced runoff water supply of gullies in Kinshasa. The computation of the runoff coefficient needs an infiltration envelope, established on site during a period of interest, and a local pluviogram decomposed in pluviophases. Rainfall simulation is carried out in 35 representative urban sites located in gully runon areas to establish a site-specific infiltration envelope. The runoff coefficient of the 35 sites is calculated for 25 geomorphologically active rains recorded between 1975 and 2012. The results show that several site-specific characteristics control runoff coefficient. The first factor is the over-compaction of the soil. Earthen roads show a runoff coefficient of 96.0 %. The second factor is the presence of a lichen seal. Bare loose soil only colonized by a lichen seal shows a runoff coefficient of 40.7 %. For the other sites, the runoff coefficient is inversely proportional to the percentage of vegetation soil cover, a normally compacted bare soil having a runoff coefficient of up to 30 %, parcels with high grass or cultures providing complete coverage showing no runoff at all. However, mowed lawns develop an impervious root mat close to the surface and, therefore, do not follow this rule: They quickly produce runoff similar to the bare and compacted surfaces. Finally, the factor slope gradient is involved. The differences due to vegetation cover disappear gradually with decreasing slope. Below a slope gradient of 0.08 m m^{-1}, the runoff coefficient is null on a bare surface. Currently, the critical rainfall for gullying in the high town of Kinshasa is 24.9 mm with a mean intensity of 21.8 mm h^{-1}. Roads generate by far most runoff and, therefore, are considered as the primary reason for gullying. The other soil uses lead most

✉ Jan Moeyersons
jan.moeyersons@africamuseum.be

[1] Department of Earth Sciences, Royal Museum for Central Africa, Tervuren, Belgium

[2] Laboratoire de Géomorphologie et Télédétection, Centre de Recherches Géologiques et Minières (CRGM), Kinshasa, Democratic Republic of the Congo

[3] Département des Sciences de la Terre (Géographie-Géologie), Faculté des Sciences, Université de Kinshasa, Kinshasa, Democratic Republic of the Congo

Published online: 18 June 2015

of the time to much smaller runoff coefficients, but their relative contribution to the supply of gullies grows with rainfall increase in height and intensity. The results provide material for gully management and adaptation strategies and open perspectives for the development of an early warning system in the region of Kinshasa. The method shows potential for being applied in other urbanized environments.

Keywords Gullying · Infiltration envelope · Rainfall simulation · Runoff coefficient · Soil use · Kinshasa

Abbreviations

IfE	Infiltration envelope
IfC	Infiltration capacity
RC	Runoff coefficient
RH	Rainfall height
RI	Rainfall intensity
SIfC	Saturated infiltration capacity
SRI	Simulated rainfall intensity
TP	Time to ponding
TR	Time to runoff

1 Introduction

Land-use/land-cover changes due to urban extension lead to changes in hydrological processes (Ferreira et al. 2012) and are the most important factors influencing gully erosion (Garcia-Ruiz 2010; Nadal-Romero et al. 2013). This is particularly true in the high town of Kinshasa (Fig. 1), where gullying poses a major economic and environmental problem (Makanzu Imwangana et al. 2012). Mega-gullies (>5 m wide) (Fig. 2) develop within the urbanized perimeter of the high town of Kinshasa 5–10 years after incipient urbanization (Makanzu Imwangana et al. 2014a, b).

Van Caillie (1983) indicated that gullying in Kinshasa could be prevented by taking runoff reducing measures in the gully runon area so that runoff discharges, critical to gully head incision, would not develop. His idea was to prevent or at least to delay headward gully growth by reducing or even annihilating runoff production in the areas draining to the gully heads. In this way, gullies should not reach their natural equilibrium state governed by the decreasing size of the runon area during headward retreat (Graf 1977). Van Caillie (1983) considered the house roofs and the hard surfaces of the courtyards critical runoff producers. But the studies of Makanzu Imwangana et al. (2014a, b) show that 91 % of the mega-gullies are not linked to houses or courtyards but to urban structures: In the first place, roads, tarred or not, with or without side-road trenches, further gutters in all forms and materials from concrete to sand but not linked to a road, also foot paths and all other artificial runoff drainage lines. Forty-four percent of the mega-gullies, fed by these structures, are axial gullies (Makanzu Imwangana et al. 2014b), which develop right upon these structures and destroy them in the same time. Makanzu Imwangana et al. (2013) conclude that every mega-gully is directly or indirectly induced by human activities. In Kinshasa, gully mitigation techniques, including biological slope protection (based on, e.g., Prosser and Slade 1994) and huge engineering constructions, have proved to be successful

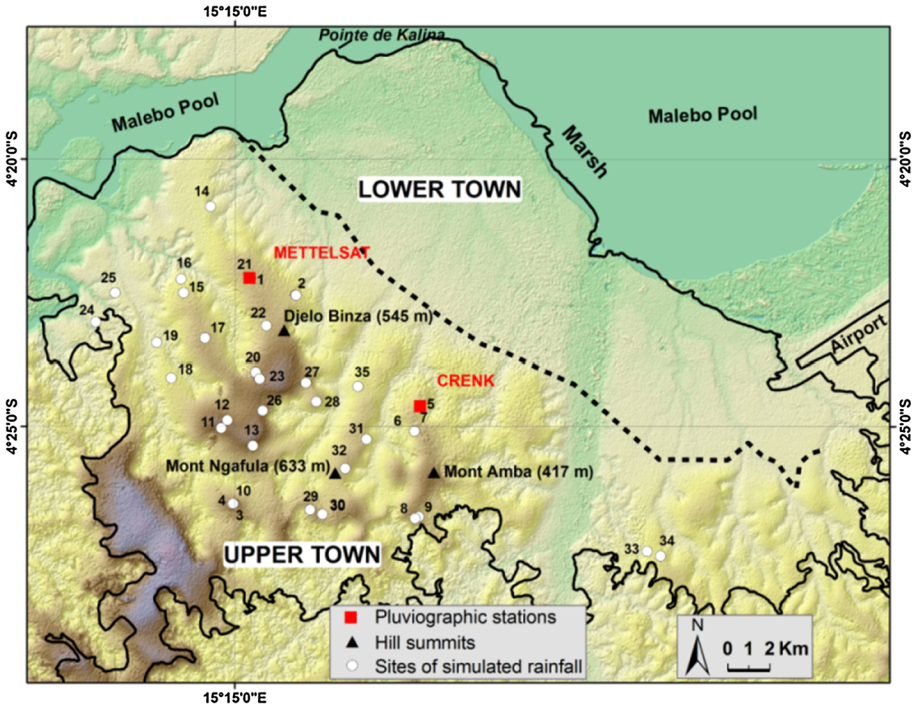

Fig. 1 Main urban zone of Kinshasa. The hilly region is delimited to the North by the *dashed line*. The *dashed line* was the southern extent of the agglomeration in the middle of the 1960s. In 2007, the hilly region is completely urbanized. The 2007 southern extent of the town, indicated by the *full line*, has shifted southward and coincides with the string of erosion cirques which limits the hilly country to the south. Mega-gullies are dispersed over the high town of Kinshasa. Sites subjected to rainfall simulation. *1* Laloux/Bord route, *2* Laloux/Route, *3* Maman Mobutu/1, *4* Maman Mobutu/2, *5* ERAIFT, *6* V.D. Funa/1, *7* V.D. Funa/2, *8* Cogelos/Parcelle, *9* Cogelos/Route, *10* Maman Mobutu/3, *11* Wamu, *12* Masikita, *13* Ngamba, *14* Lycée Tobogisa, *15* Bois de Ndangye, *16* Jardin du Graal, *17* Sanga Mamba, *18* Buadi, *19* Kibambe, *20* Djelo Binza, *21* METTELSAT, *22* Secteur Météo, *23* EDAP/UPN, *24*: Koweit, *25* Don Bosco, *26* Kingu, *27* Matiata, *28* De la Paix, *29* Bianda/1, *30* Bianda/2, *31* Mazamba, *32* Masanga Mbila, *33* Kimbasenke/Bord rue, *34* Kimbasenke and *35* Ngafani

to a certain degree (Makanzu Imwangana 2010; Makanzu Imwangana et al. 2013, 2014a, b). But nevertheless, gully occurrence remains difficult to predict in space and time. Makanzu Imwangana et al. (2014b) show that most gullies are not 'valley'-gullies. Therefore, digital terrain models, based on topographical water flow convergence (Prosser and Dietrich 1995; Dewitte et al. 2015), cannot be used to predict the location of future channel heads.

The aim of this work is to find out more about the absolute and relative contribution of the most characteristic soil uses/covers in Kinshasa to the runoff supply of the mega-gullies. In this way, critical runoff contributor sites to gullying can be better discriminated.

To achieve this goal, we need to assess the runoff coefficient in a sector with homogeneous soil, vegetation and slope gradient characteristics. It is, however, logistically nearly impossible to install in the middle of Kinshasa several permanent field setups to measure Horton runoff (Horton 1945; Ben-Asher and Humborg 1992). To our knowledge, no method exists to assess the site- and rainfall-specific runoff coefficient (RC) at an arbitrary place so that the amount of runoff delivered by one place can be compared with

Fig. 2 Mega-gully 'Laloux' has incised Avenue Bolivar over a distance of 2129 km, is about 90 m wide and 30 m deep. The houses, formerly at a certain distance from the street, will slide into the mega-gully as it deepens and widens. In the close foreground, a metallic construction meant to stop headward retreat of the gully head

the amount of runoff by another place for the same rain. Therefore, to meet the aim of this work, we propose a new method of site- and rainfall-specific assessment of RC. Literature provides a wealth of studies, most by means of rainfall simulation (e.g., Casenave and Valentin 1992; Dunne et al. 1991; Roth 2004). These studies focus on soil surface characteristics and vegetation as factors governing infiltration capacity (IfC) and have inspired us to use rainfall simulation technology to provide data to the mathematical model of IfC by Smith (1972). In this way, we are able to evaluate rainfall characteristics as another factor governing IfC.

2 Study area

The town of Kinshasa knew its first development in the rather flat plain (280–300 m ASL) along the shore and the marshes of the Malebo Pool (Fig. 1). At the end of the 1960s, the whole plain from Pointe de Kalina to the west and the Tshangu basin close to the airport to the east was occupied. The southern limit of the city at that time (Fig. 1) coincides with the northern edge of an undulating and widely dissected plateau, whose summits culminate between 350 and 710 m ASL (De Maximy 1978; De Maximy and Van Caillie 1978). The plateau extends over 240 km^2 and is delimited to the south by a continuous sequence of spring amphitheaters as indicated in Fig. 1. This explains the irregular and curved planform of the southern plateau border. The northern edge of the plateau is believed to be an ancient cliff or bluff of the Malebo Pool (De Maximy 1978). Both the plateau and adjacent northern and southern plains are underlain by a sub-horizontal series of reddish shale and soft sandstone of questionable Mesozoic age (Egoroff 1955). On the plateau, this series is overlain by a 50- to 100-m-thick layer of sands belonging to the series of ochrous sands, dating either to the end of the Cretaceous or to mid-Tertiary times (Cahen 1954) and considered by De Ploey (1963) as a Kalahari sand type. The hills show a typical convex form and are etched out in these sands. The valleys between the hills correspond more or less to the top of the underlying shale-soft sandstone series, which acts as an aquitard

compared to the porous overlying sands. Therefore, all the hills of the plateau contain a perched water table with corresponding perennial springs at their foot (Van Caillie 1983).

The gully problem in Kinshasa started with the urbanization of the plateau at the end of the sixties of the twentieth century (Makanzu Imwangana et al. 2014b). In 2007, the whole plateau was built up. Today the town is extending further southward beyond the belt of spring amphitheaters into the lower lying plain to the south. The gullies in the high town (e.g., Fig. 2) are the result of vertical incision by concentrated wash. The incisions sometimes reach and hence drain the water table. Some of these gullies are very large (e.g., Mataba 1: 960 m long, up to 150 m wide and up to 50 m deep), damage infrastructure and develop within a few hours.

A relationship between gully shape and hydro-geological conditions in the high town seems to exist. Gullies in Kinshasa have a V-like cross section as long as they remain above the perched water table (Fig. 2). In some instances, they widen and show a flat floor when they reach the latter in their lower course. Aggradation and water problems related to gully incision can impact kilometers downslope in the city.

Kinshasa has a tropical wet and dry climate (Peel et al. 2007). The rainy season spans from September/October to May (Bultot 1971). At the weather station of Kinshasa/Binza (Fig. 1), the mean annual precipitation amounts to $\sim$1400 mm (Makanzu Imwangana 2010). Ntombi et al. (2004, 2009) indicate by statistics that the global change in the Kinshasa region may be expressed in the future by increased rainfall, both in height and in intensity.

The natural vegetation of the Kinshasa region is composed of dry dense forest, savannahs and semi-aquatic and aquatic formations in the valleys and around the Malebo Pool (Pain 1984; Kikufi and Lukoki 2008). In town, nothing remains from this luxurious vegetation besides a few grasses like *Laudetia demeusi* and *Schyzochysium semiberle* (Tshibangu et al. 1997). This change from natural vegetation conditions did, however, not trigger gullying processes.

The population of Kinshasa increased by a factor of 20 in the last 50 years (Hôtel de Ville de Kinshasa 2007) and is now over nine million. In the meantime, the surface of the urbanized area grew by a factor four and is now over 440 km^2 (Makanzu Imwangana et al. 2012).

3 Materials and methods

The RC assessment method is based on Smith (1972) who presents a mathematical simulation of the infiltration envelope (IfE) and the time decay curve of the infiltration capacity (IfC) of loose soils. IfE encompasses all IfC graphs for all initial rainfall intensities higher than the saturated infiltration capacity (SIfC) (Fig. 3) and is expressed by the power equation:

$$\mathrm{IfE} = \mathrm{SIfC} + a(T)^{-b} \tag{1}$$

where a and b are to be defined in function of time T. SIfC is a site-specific value.

According to Smith (1972), the time decay curve of the IfC obeys to the equation:

$$\mathrm{IfC} = \mathrm{SIfC} + m(T)^{-n} \tag{2}$$

where m and n are to be defined in function of time T.

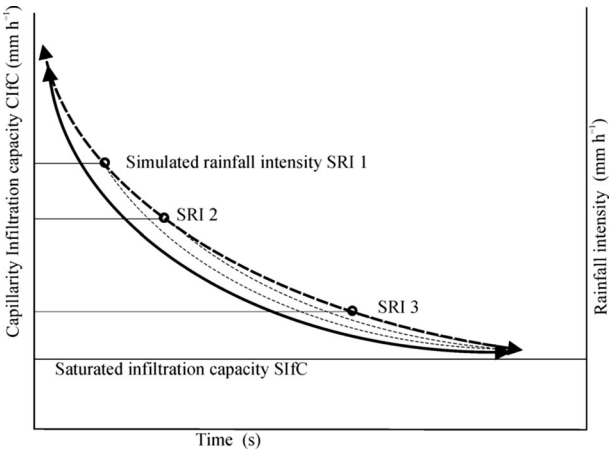

Fig. 3 Full line represents the infiltration capacity (IfC) by Horton (1933) versus time for the case that rainfall intensity (RI) is so high that ponding occurs at Time = 0. Horton infiltration capacity is composed of capillarity infiltration capacity, decaying with time and saturated infiltration, remaining constant. Small dashed lines represent the full line, displaced to the right to cross the respective points of ponding (TP) at simulated rainfall intensity (SRI). The *dashed line* is called the infiltration envelope (IfE). It is composed of all possible TP points

Contrary to Smith (1972) who uses mathematical simulation to provide IfE data, data input in this work is derived from field and laboratory observations by means of a rainfall simulator and site-specific IfE estimations, representing the most current soil uses/covers. Further, the RC is calculated for geomorphologically active rainstorms, being recorded since 1989 in Kinshasa.

This work illustrates another possibility of rain simulator use in hydrological, pedological and geomorphic research (Martinez-Murillo et al. 2013). Rain simulation is applied for the direct measurement of runoff and erosion (Lasanta et al. 2000; Römkens et al. 2001; Hamed et al. 2002; Arnaez et al. 2004) and for the empirical study of processes under conditions as close as possible to the natural ones. Rainfall simulation is also used to assess the total infiltration capacity during a simulated rainstorm and to define indirectly the total RC for the totality of the event (Esteves et al. 2000; Duiker et al. 2001; Poulenard et al. 2001; Li et al. 2011). But these experiments do not consider the time dependency of the infiltration capacity in capillary soils as already defined by Horton (1933). In this study, a rain simulator is used as an infiltrometer. Moeyersons (1989) defined in Rwanda for the first time a field IfE by means of a drip screen rainfall simulator, but he only classified sites in function of their time to ponding (TP), supposing an inverse relation between TP and RC. This study goes a step forward and assesses directly site- and rainfall-specific RC.

3.1 Computation method of a site- and rainfall-specific RC

A rainstorm is decomposed in pluviophases, i.e., small packages of the same precipitation volume or rainfall height (RH) (Fig. 4). According to Smith (1972), a natural rainstorm with one runoff producing rainfall intensity (RI) peak can be subdivided into three parts. The first part concerns the wetting phase of the soil between the start of rainfall and the moment when water ponds (time to ponding: TP) at the soil surface (Fig. 4). Soil wetting is

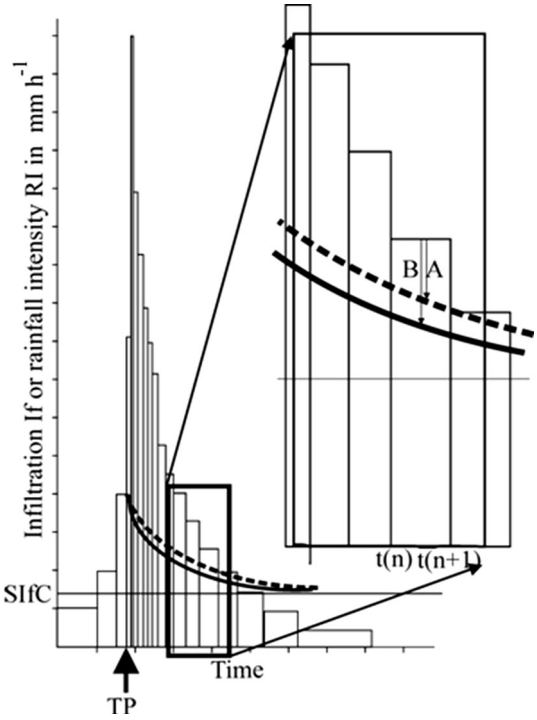

Fig. 4 Illustration of the computation of the site-specific runoff coefficient (RC) for a given rainstorm, decomposed in pluviophases of the same rainfall height (RH). Construction of the IfC decay curve at the moment of TP/TR. The IfE decay curve represented by the *dashed line* is used as a proxy for the IfC decay curve. Explanation in text

due to capillary suction and no runoff occurs. According to Smith (1972), ponding and subsequent decay of the infiltration capacity (IfC) start at very nearly the time when accumulated volume of infiltrated water reaches a value which is associated with the particular rainfall intensity at the time of ponding (TP), as given by the site-specific IfE. This volume, or rainfall height, needed to produce runoff (expressed in mm), can be calculated on the basis of the IfE by multiplying TP by its respective RI.

The second part of the rainstorm generates runoff and starts at TP (Fig. 4). From the top of the pluviophase leading to an excess between RI and infiltration, the time decay curve of the infiltration capacity (IfC) can be constructed. This curve is represented by the full line in Figs. 2 and 3. The TP is arbitrarily set at the end of the first pluviophase leading to runoff (Fig. 4). The second part is the runoff generating phase of the rainstorm. The total amount of runoff generated during a rainstorm is theoretically given by the cumulated difference between RI and IfC for all the pluviophases where RI $\geq$ IfC.

The third part of the rainstorm concerns the pluviophases where RI $\leq$ IfC. No more runoff is produced on the site, although remnant axial runoff can be present in the landscape. The runoff coefficient (RC) is the total runoff produced during part two of the storm divided by the total rainstorm rainfall height (RH) and varies between 0 and 1 or between 0 and 100 %.

A natural rainstorm can show several subsequent peaks where RI $\geq$ SIfC, leading to alternative periods of runoff and no runoff production. There is no reason to reconstruct the time decay curve of the IfC at the consecutive moments of runoff appearance, because it is supposed that during the same rainstorm, the soil does not significantly dry out and that capillary tension remains at the level of the former runoff producing RI peak. Therefore,

the computation of the RC for a rainstorm with consecutive alternations of periods with and without runoff generation is done in reference to the IfC time decay curve, constructed from the top of the first runoff producing pluviophase of the rainstorm.

3.2 Rainfall simulator

The rainfall simulator used in Kinshasa is manufactured at the Laboratory of experimental geomorphology at the KU Leuven, Belgium (Fig. 5). The instrument is of the sprinkler type and functions by means of three valves: Two valves produce a SRI of 35 mm h^{-1} each, whereas the third generates a SRI of 70 mm h^{-1}. The circular impluvium of the apparatus has a diameter of ± 3 m resulting in an area of ~ 7 m^2. A water reserve of 500 l is taken into the field. An electric generator Honda EC2000 drives the pump. At the time of construction, the simulator produces effectively SRI values of respectively 35, 70, 105 and 140 mm h^{-1}. But, in the field, the SRI values are sometimes aberrant and unstable in time. Therefore, the SRI has to be measured during every rain simulation test. Otherwise, marked differences of SRI inside the ~ 7 m^2 impluvium cannot be observed.

3.3 Tested sites, procedures and additional data collection

Thirty-five sites have been selected for simulated rainfall tests (Fig. 1). In doing so, the sites represent the most common soil uses/covers in the high town of Kinshasa. Included are different types of earthen roads, courtyards, cultivated parcels, not cultivated spaces,

Fig. 5 KU Leuven rain simulator deployed in the ERAIFT site. The wetted impluvium is visible in the foreground

Table 1 Characteristics of sites subjected to rainfall simulation

Site no.	Site name	Site description	Soil cover (%)	Type of vegetation
1	Laloux/Bord route	Road side with sparse vegetation	5	*Boerrhavia diffusa, Digitaria longiflora*
2	Laloux/Route	Unpaved road, bare soil	0	
3	Maman Mobutu/1	Grass in garden	40	*Digitaria horizontalis, Eragrostis ciliaris, Tridax procumbeus*
4	Maman Mobutu/2	Tall grass in fallow land	60	*Digitaria horizontalis*
5	ERAIFT	Cultural area with Lichens on soil surface	14	*Hibiscus sabdarrifa, Hibiscus acetocella*
6	V.D. Funa/1	Land inhabited	1	*Croton hirtus, Cyperus* sp.
7	V.D. Funa/2	Grassy field (Tall grass)	50	*Hyparrhenia familiaris, Digitaria horizontalis, Pennisetum polystaschyon*
8	Cogelos/Parcelle	Houseyard	50	*Cynodon dactylon*
9	Cogelos/Route	Unpaved road, bare soil	0	
10	Maman Mobutu/3	Dense Grass in garden	90	*Paspalum notatum, Digitaria horizontalis, Mariscus aletrnifolius, Cyperus distans*
11	Wamu	Sparse vegetation in land inhabited	50	*Paspalum notatum, Eleusine indica, Cynodon dactylon*
12	Masikita	Street with grass	50	*Panicum maximum, Eleusine indica*
13	Ngamaba	Road side with grass	30	*Cynodon dactylon, Cyperus* sp.
14	Lycée Tobongisa	Sparse vegetation, land inhabited	5	*Cynodon dactylon, Panicum repens*
15	Bois de Ndangye	Road side with sparse vegetation	8	*Heterotis rotundifolia, Schweinckia americana*
16	Jardin du Graal	Grass in garden	30	*Digitaria horizontalis, Scweinckia americana*
17	Sanga Mamba	Grass in land inhabited	55	*Cynodon dactylon*
18	Buadi	Tall grass in land uninhabited	30	*Eragrostis tremula, Croton hirtus*
19	Kibambe	Sparse vegetation, land inhabited	15	*Cynodon dactylon*
20	Djelo Binza	Garden with grass	90	*Eleusine indica, Cynodon dactylon, Paspalum notatum*
21	Mettelsat	Sparse vegetation in garden	10	*Schweinckia americana*
22	Secteur Météo	Garden with grass	100	*Paspalum notatum, Eleusine indica*
23	EDAP/UPN	Bare soil	0	
24	Koweit	Field lying fallow	15	*Cynodon dactylon, Digitaria horizontalis*
25	Don Bosco	Dense grass in playground	90	*Cynodon dactylon, Eleusine indica*
26	Kingu	Tall grass in uninhabited land	60	*Eleusine indica*
27	Madiata	Cultural area	2	*Manihot esculenta*

Table 1 continued

Site no.	Site name	Site description	Soil cover (%)	Type of vegetation
28	De la Paix	Dense Grass in road side	80	*Cynodon dactylon, Eleusine indica*
29	Bianda/1	Sparse vegetation in land inhabited	3	*Urena lobata, Croton hirtus*
30	Bianda/2	Sparse vegetation, land inhabited	40	*Digitaria horizontalis, Eragrostis tremula*
31	Mazamba	Bare soil in inhabited land	0	
32	Masanga Mbila	Grass in garden	50	*Paspalum notatum*
33	Kimbanseke/Bord Rue	Road side with tall grass	60	*Cynodn dactylon, Triumfetta rhomboidea, Senna occidentalis*
34	Kimbanseke/ Parcelle	Unpaved area, bare soil	0	–
35	Ngafani	Street with grass	40	*Eleusine indica*

wild grasses, lawns and bare soil parts. A short description of the vegetation cover is given for every site, and the soil coverage percentage is estimated visually, at the real surface of the soil, at the base of the vegetation. The sites are listed with their name, soil affectation, percentage of soil coverage by vegetation and vegetation specification in Table 1.

The tests took place on slope gradients varying between 0 and 0.02 m m^{-1}. This range is representative of the runon areas of the mega-gully heads. In the field, the 35 sites were tested for field infiltration capacity by means of a ring infiltrometer. Dry bulk density, water content, porosity, SIfC and granulometric composition of the soil were obtained in the laboratory. For this purpose, volumetric sampling was applied. Soil samples of a constant volume (240 cm^3) have been retrieved by means of a PVC tube (Moeyersons (1989). The tube has to be inserted into the soil till the 240 cm^3 indication (Fig. 5). The soil sample of 240 cm^3 can be retrieved by slightly turning the tube and slowly elevating it. The disturbed sample is kept in a plastic bag for weighing in the laboratory before and after drying. Sometimes, part of the soil embraced by the PVC tube remains in the bottom of the hole after sampling. In this case, the small heap in the bottom of the sample hole is recuperated manually by a trowel or a slice. The volume precision by this sampling method is in the particular case of the Kalahari sands of Kinshasa 240 ± 5 cm^3. The original volume of the soil sample and its dry and wet (field) weight allow calculating the wet and dry bulk density of the soil and the water content in the field. The specific weight of the Kalahari sand (2.67 g cm^{-3}) was defined by picnometer test (Moeyersons 1978) and allows calculating the in situ porosity and water saturation of the soil.

Particle size analysis of soil samples was carried out according to the method of 'Service Pédologique interafricain.' The oven-dried sample is passed first through a standard series of sieves (2000–63 μm) and then washed through a filter paper of 12–14 μm.

Infiltration capacity measurements were conducted in the field and in the laboratory. In the field, the PVC tube described above was used as a ring infiltrometer. All measurements have to be done in places where the tube, displaying a sharpened edge, can be pushed into the ground without sediment disturbance. This excludes measurements where roots are

Table 2 History of rainfall simulation tests and of soil characteristics

Site no.	Site name	Impluvium	Simulated rainfall intensity (mm h^{-1})	TR (s)	Soil water content (%)	Dry bulk density (g cm^{-3})	Particle size class	SIfC in laboratory (permeameter)
1	Laloux/Bord Route	1	55	225	11	1.6	2	168
		2	110	58	13	1.6		
		3	174	20	15	1.6		
2	Laloux/Route	1	236	7	6	1.9	3	0
		2	154	9	–	–		
		3	47	47	–	–		
3	Ma Mobutu I	1	54	450	29	1.4	2	373
		2	157	210	28	1.4		
		3	205	155	16	1.3		
4	Ma Mobutu II	1	189	>1500	20	1.7	3	115
5	ERAIFT	1	129	110	12	1.5	3	160
		1	287	50	–	–		
		1	287	20	7	1.5		
		2	104	174	13	1.5		
		2	116	94	15	1.7		
		2	138	70	8	1.6		
		3	34	170	15	1.4		
		3	36	166	14	1.4		
		3	156	45	–	–		
		3	245	45				
6	Versant droit Funa I	1	45	1320	16	1.5	2	236
		2	224	75	8	1.5		
		3	157	190	19	1.5		
		3	110	30	15	1.5		
7	Versant droit Funa II	4	236	616	21	1.3	3	249
		5	205	1102	22	1.4		
8	Cogelos/ Parcelle	1	58	1890	19	1.5	3	160
		2	227	230	18	1.7		
		3	312	174	20	1.5		
9	Cogelos/Route	1	51	84	14	1.6	3	115
		2	170	41	11	1.5		
		3	214	31	13	1.6		
10	Ma Mobutu III	1	44	>437	16	1.5	3	160
		2	134	619	30	1.4		
		3	236	150	24	1.6		
		4	132	347	26	1.6		

Table 2 continued

Site no.	Site name	Impluvium	Simulated rainfall intensity (mm h^{-1})	TR (s)	Soil water content (%)	Dry bulk density (g cm^{-3})	Particle size class	SIfC in laboratory (permeameter)
11	Wamu I	1	47	290	16	1.5	3	115
		2	105	125	15	1.5		
		3	195	61	14	1.5		
	Wamu II	1	178	167	16	1.6	3	115
		2	112	230	17	1.7		
		3	47	701	18	1.5		
12	Masikita	1	47	160	15	1.4	2	236
		1	135	65	24	1.2		
		1	220	59	16	1.6		
		2	36	>600	21	1.6		
		2	126	125	27	1.5		
		2	220	110	27	1.5		
		3	210	56	13	1.6		
		3	126	86	16	1.5		
		3	46	197	17	1.8		
13	Ngamaba I	1	77	516	16	1.4	3	115
		1	126	294	19	1.5		
		1	230	124	19	1.6		
	Ngamaba II	1	50	731	16	1.6	3	115
		1	233	16	16	1.6		
		2	47	180	16	1.6		
		2	135	70	17	1.6		
14	Lycée Tobongisa	1	50	672	25	1.2	2	373
		1	170	110	24	1.4		
		1	362	6	23	1.4		
		2	320	107	21	1.4		
		2	164	178	25	1.4		
		2	47	>1097	26	1.5		
15	Bois de Ndangye	1	39	289	8	1.3	2	304
		1	153	53	12	1.7		
		1	312	47	12	1.7		
		2	53	340	10	1.4		
		2	167	56	14	1.2		
		2	208	52	29	1.2		
16	Jardin du Graal I	1	44	720	15	1.8	1	116
		2	148	384	18	1.8		
		3	224	173	20	1.5		
	Jardin du Graal II	1	243	82	17	1.6	1	116
		2	113	166	17	1.5		

Table 2 continued

Site no.	Site name	Impluvium	Simulated rainfall intensity (mm h^{-1})	TR (s)	Soil water content (%)	Dry bulk density (g cm^{-3})	Particle size class	SIfC in laboratory (permeameter)
17	Sanga Mamba I	1	50	>672	20	1.5	2	304
		2	129	210	36	1.2		
		3	208	102	35	1.3		
	Sanga Mamba II	1	240	74	16	1.7	3	304
		2	126	176	17	1.6		
		3	48	258	12	1.4		
18	Buadi	1	50	>611	15	1.3	2	236
		2	113	>645	17	1.6		
		3	205	>505	23	1.6		
19	Kibambe	1	58	793	19	1.6	1	234
		2	173	160	17	1.5		
		3	230	125	16	1.4		
20	Djelo Binza I	1	118	117	12	1.2	3	294
		2	58	178	22	1.3		
		3	238	59	18	1.3		
	Djelo Binza II	1	198	68	20	1.1	3	294
		2	284	56	14	1.3		
		3	50	180	11	1.2		
21	Mettelsat	1	42	>603	15	1.5	2	304
		2	135	422	22	1.4		
		3	236	242	22	1.6		
22	Secteur Météo	1	187	56	25	0,9	1	470
		2	221	80	24	1.0		
		3	55	239	23	1.0		
23	EDAP/UPN	1	189	300	13	1.1	2	441
		2	205	138	20	1.4		
		3	52	>546	15	1.3		
24	Koweit	1	268	56	17	1.0	1	352
		2	230	248	24	1.5		
		3	60	1335	24	1.4		
25	Don Bosco/ Kimbwala	1	55	220	19	1.0	1	470
		2	177	96	26	0.9		
		3	217	76	21	1.0		
26	Bukamikuwa	1	55	>474	17	1.3	1	293
		2	202	>542	24	1.3		
		3	250	213	20	1.4		
27	Madiata	1	66	>356	17	1.2	1	234
		2	170	183	21	1.5		
		3	230	80	24	1.5		

Table 2 continued

Site no.	Site name	Impluvium	Simulated rainfall intensity (mm h^{-1})	TR (s)	Soil water content (%)	Dry bulk density (g cm^{-3})	Particle size class	SIfC in laboratory (permeameter)
28	De la paix	1	231	47	18	1.4	3	205
		2	87	>496	18	1.6		
		3	126	73	17	1.4		
29	Bianda I	1	87	>612	17	1.4	3	160
		2	150	900	22	1.5		
		3	240	300	20	1.7		
30	Bianda II	1	240	87	14	1.4	2	236
		2	129	519	20	1.5		
		3	71	>621	13	1.5		
31	Mazamba	1	78	186	11	1.2	3	205
		2	134	116	11	1.5		
		3	227	31	9	1.4		
32	Masanga Mbila	1	51	>510	14	1.5	3	249
		2	136	100	19	1.3		
		3	241	40	27	1.3		
33	Kimbanseke/ Rue	1	78	>607	20	1.6	2	304
		2	137	>434	31	1.3		
		3	211	164	13	1.4		
34	Kimbanseke/ Parcelle	1	97	80	10	1.3	2	373
		2	106	100	16	1.3		
		3	227	36	18	1.4		
35	Ngafani	1	42	>372	18	1.5	2	236
		2	126	186	19	1.5		
		3	230	135	23	1.7		

present. The IfC (Darcy 1856) is defined by the timing of the fall of water level in the tube above the ground and is given by Eq. 3 (Lambe and Whitman 1979):

$$k = \frac{2.3 \times a \times L \times \log_{10}(h_0)}{A(t_1 - t_0) \times h_1} \tag{3}$$

where k is the permeability in cm s^{-1}, a is the section of the tube, which is 48 cm^2, L is the thickness of the sample tested, which is 5 cm, the depth to which the infiltrometer is inserted in the ground without disturbance, $A = a$ is the section of the sample tested, which is 48 cm^2, $t_1 - t_0$ is the time in seconds of the fall of water level h_0 (=20 cm) to h_1 (=5 cm).

For the PVC tube ring infiltrometer in question, the infiltration capacity is given by:

$$k = 6.93/(t_1 - t_0) \tag{4}$$

In the laboratory, a constant head permeameter was used to test SIfC of soil samples of the tested sites. SIfC was defined in function of the dry bulk density.

The exact chronological procedure of rain simulation, number of impluvia tested, measurements of hydraulic conductivity, volumetric sampling varies from site to site and is given in Table 2. In most sites, a rainfall test has been done in three different impluvia in order to establish the IfE. But the procedure was flexible. In some sites (5, 12, 13/1, 14 and 15), the same impluvium was used for repeated tests, in order to verify the influence of soil moisture on the TP test. In other cases, the influence of vegetation cover was addressed.

3.4 Active rainstorm data gathering

In nine districts situated within a distance of 1 km to the weather station of Kinshasa/Binza (Fig. 1), an investigation was carried out among the civil authorities and the inhabitants. The aim was to obtain the exact dates (day, month and year) of sudden mega-gully initiation and/or development. The pluviograms of the geomorphologically active rainfalls linked to these occurrences are provided by the National Agency of Meteorology (METTELSAT, Fig. 1). However, the analog cumulative rainfall height (RH) graphs do not allow a very precise decomposition of a rainfall into pluviophases, i.e., packages of equal RH. The 23 rains were decomposed manually into pluviophases of 5 mm RH. The definition of the rainfall intensity (RI) of each pluviophase is rather approximate once RI exceeds a few tens of mm h^{-1}. For this reason, an electronic pluviograph (Station ALCYR) was installed at CRENK/Mont Amba (Fig. 1). The instrument is of the tipping bucket type and measures the time in seconds between every package of RH of 0.2 mm.

4 Results

4.1 Soil parameters of the Kalahari sands

The particle sizes of the 35 tested soils show only minor differences. In average, the Kinshasa sands contain 97.7 % sand (>63 μm). The mean D_{10} amounts to 100 μm. Based on the spread of the granulometric population, three classes of samples are considered: the class with 95.2–97.1 % sand (Class 1), the class with 97.1–98.1 % sand (Class 2) and the class with 98.2–99.1 % sand (Class 3). Table 2 indicates the granulometric class of every site.

In the 35 sites, the upper 5 cm of the soil has an initial water content varying between 2 and 39 % with a mean value of 9 %. The volume porosity varies between 33 and 65 % with an average of 50 %. This high value is due to roots and other fine humic material. The initial soil saturation varies between 5 and 85 % with an average of 25 %. The dry bulk density varies between 1 and 1.9 g cm^{-3} with a mean of 1.4 g cm^{-3}.

The ring infiltrometer tests prior to the first rainfall simulation show site-specific IfC ranging from <50 to more than 900 mm h^{-1}. There exists in the field no correlation between IfC and dry bulk density. The laboratory tests with constant head permeameter (Fig. 6) show that SIfC varies between 0 mm h^{-1} for a dry bulk density >1.85 g cm^{-3} and 200–260 mm h^{-1} for a dry bulk density of the order of 1.4–1.5 g cm^{-3}, according to the granulometric class. The difference between field and laboratory permeability test can be ascribed to the unsaturated state of the soil at the start of the field test. For this reason, a component of succion by capillarity is added to the saturated conductivity or SIfC (Moeyersons 1989). Only the latter is measured in the laboratory.

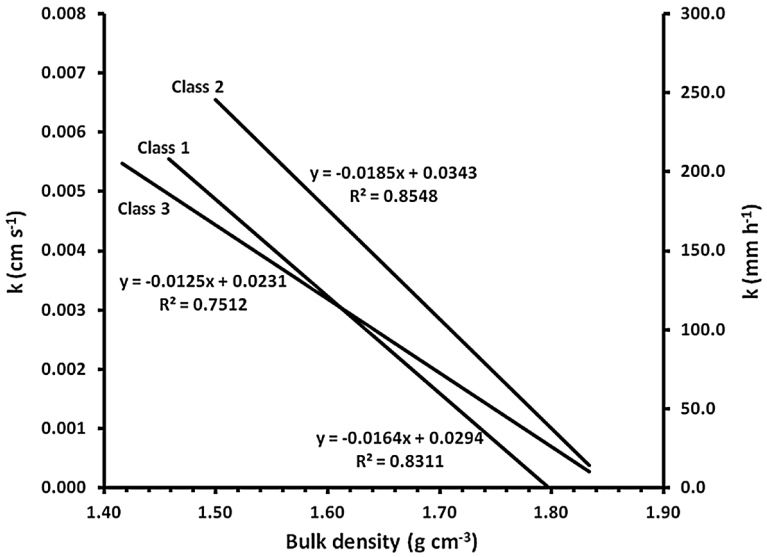

Fig. 6 Saturated infiltration capacity (SIfC = k) measured in the laboratory by a permeameter with constant head, for the three classes of 'Kalahari' sands mentioned in the text; Y = SIfC; X = dry bulk density

4.2 Infiltration envelope parameters of 35 sites

Unlike in the mathematical simulation by Smith (1972), Eq. (2) cannot be time-normalized on the basis of the Kinshasa field data. Therefore, the IfE time decay curve (dashed line in Figs. 3, 4) corresponding to Eq. (1) is used as a proxy for the IfC decay curve of Eq. (2). Figure 3 shows a decreasing deviation between IfC and IfE with decreasing values of initial RI or simulated RI (SRI). For the Kinshasa sands, the range between maximum IfC and SIfC is very high. The maximum IfC value, giving rise to immediate ponding (TP = 0), can be derived from the observation made during tests with Kalahari sands (Moeyersons 1978) that at the very start of rainfall upon a dry surface, the first raindrops are absorbed by the sand without leaving an impact crater. This indicates that the first raindrops are sucked into the ground at the speed of their impact velocity. The latter should be equal to the final fall velocity of a mean raindrop which is of the order of 30.10^6 mm h^{-1} (Laws 1941). The range of SRI to define the IfE in 35 sites varies between 250 and 35 mm h^{-1} and should fall in the lower sector of Fig. 3, where IfE and IfC tend to coincide. Nevertheless, there remains the theoretical possibility that the runoff volume during pluviophase $[t(n); t(n + 1)]$ as defined by the IfE (dashed line on Fig. 4) is slightly smaller than the runoff volume as defined by the IfC decay curve $\{t(n + 1) - t(n)\}B > \{t(n + 1) - t(n)\}A$ (Fig. 4).

4.2.1 Input 1: infiltration envelope

The calibration of an infiltration envelope (IfE) necessitates the determination of at least three TP points in a logarithmic RI–TP-graph and the knowledge of SIfC. This allows the construction of a power trend line asymptotic to SIfC. The portable rainfall simulator,

described in Sect. 3.2, was used to determine the three points (Fig. 3). For points 2 and 3, the rainfall simulator has to be displaced to another impluvium where slope gradient, vegetation/soil use and cover are closely identical and where the water content in the 5 upper cm of the soil is not influenced by the former test.

During the campaign, it soon appeared that a unequivocal determination of TP was not possible. Ponding at the surface never occurred at the same time in the entire impluvium. Some parts remained dry, while others were producing already appreciable runoff. For this reason, the IfE is established by measuring the time in seconds between the start of SRI and the moment that a runoff runnel reaches 10 cm beyond the impluvium border (time to runoff, TR). The IfE, established by TR points, is rather a runoff envelope because the TR is believed to approximate the time to continuous runoff in the field. For the sake of convenience, the term infiltration envelope (IfE) will be used further in this article. The term refers to ponding in the discussion of the mathematical model of Smith (1972) and refers to the moment of continuous runoff when discussing the rain simulation results.

In 16 sites (Nos. 1, 2, 3, 5, 6, 8, 9, 11, 16, 19, 20, 22, 24, 25, 31 and 34), three TP/TR values could be taken (Table 2). They increase with lowering SRI as it could be expected on the basis of the mathematical simulation by Smith (1972) (Fig. 3). Figure 6 shows SIfC depending on the granulometric class of the site and on the dry bulk density, measured in the constant head permeameter in the laboratory. The difficulty in determining SIfE in the field is that in most cases, SIfC in Fig. 6 (laboratory) appears to be superior to one or two or even to the three SRI values used during the rainfall tests (Table 2). The phenomenon is illustrated for the sites of Djelo Binza 1 and 2 (Fig. 7). The only exception is site 2, an earthen road at Laloux, where the dry bulk density reaches 1.9 g cm^{-3} (Table 2), which implies a close-to-zero SIfC (Fig. 6). For the 15 other sites, SIfC measured in the

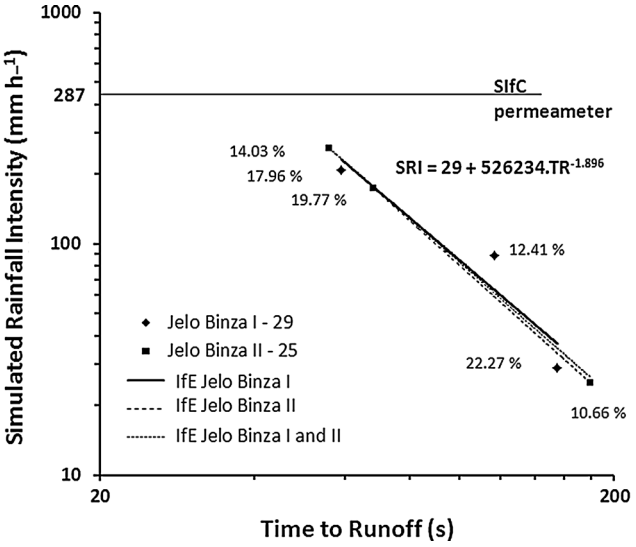

Fig. 7 Two IfE tests at the Jelo Binza sites. In spite of marked inter- and intra-site differences in water content after each test (indicated in % of water weight to total sample weight), IfEs closely coincide, indicating that other factors than capillary suction by the soil are important. The SIfC, deduced from the permeameter for the local sand class and the dry bulk density, amounts to 287 mm h^{-1}. The infiltration envelopes show that runoff occurs after a certain TR at much lower rainfall intensities

laboratory does not correspond to the SIfC values suggested by rainfall simulation tests (Table 2). In spite of all infiltrometer and permeameter measurements, valid field SIfC data are not available for the 15 sites where three SRI tests gave univocal results and where the dry bulk density remains below the critical 1.85 g cm^{-3} (Fig. 6). Therefore, in order to establish the SIfE for these sites, several procedures were applied. One method assesses the effective impluvium section as a percentage of the entire surface of the impluvium. As a criterion, the percentage of vegetation cover has been used. But it quickly appears that the recalculated SIfC is in all cases still much too high compared to the three SRIs applied to define the three TP/TR times. The reason is that in most cases, especially where grasses are concerned, the root extension just below the soil surface is much higher than the stem coverage above the soil surface. Knowing that the SIfC in equilibrium with the specific soil use/cover at every site should fall between 0 and the lowest SRI of the rainfall test, the half value of the lowest SRI of the test is arbitrarily taken as the horizontal line to which the IfE has to be asymptotic (Fig. 3).

In a double logarithmic (SRI-TR/TP) graph, IfEs of the 16 sites (1, 2, 3, 5, 6, 8, 9, 11, 16, 19, 20, 22, 24, 25, 31 and 34) are all rectilinear with a comparable slope gradient, but without being strictly parallel as in the mathematic simulation by Smith (1972). However, this allows defining an approximate IfE for the 19 other sites where TP/TR data are controversial or insufficient in number. Table 5 lists the parameters *a*, *b* and SIfC (Eq. 1) for all sites. Figure 8 shows all IEs.

4.2.2 Input 2: pluviographic data of geomorphologically active rains

Based on field investigation (Sect. 3.4), 23 hard copy pluviograms of active rains were collected at METTELSAT. The maximal mean RI during 30 min (the I30 defined by

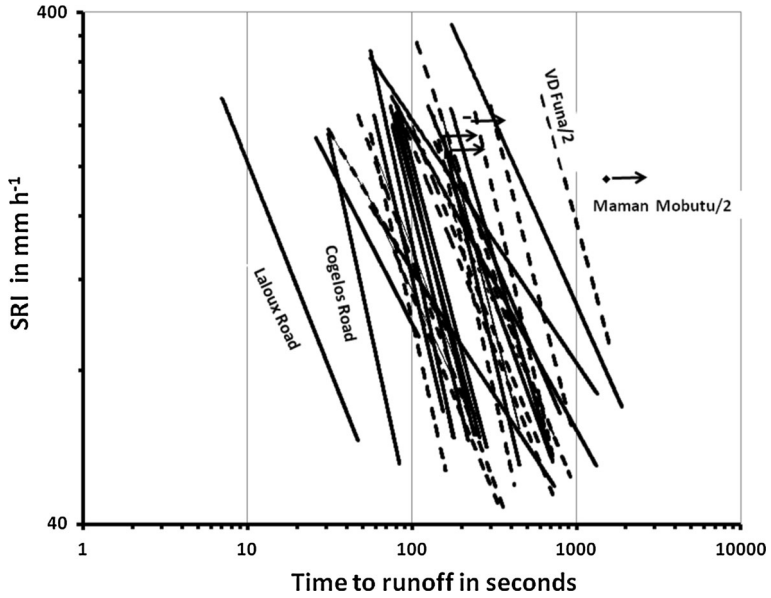

Fig. 8 IfEs as power trendlines for the 35 sites tested. *Dashed lines* indicate that the third point of the site is estimated. *Arrow* indicates that TR is not reached

Hudson (1971)) of the 23 active rainstorms was measured on these respective pluviograms. Another two rainstorms, registered by the electronic pluviograph, were added to the series, although field investigations were needed to ensure that these two rains were also active. The 25 rainstorms are all used in Sect. 4.4 to calculate RC. Their average RH attains 64 mm, and their mean RI is 37 mm h^{-1} (Table 3).

Table 4 shows the active rainstorms with the lowest (24.9 mm) and the highest (118.5 mm) RH decomposed in their respective pluviophases. Also, a rainstorm from the middle of the cluster (67 mm) is added. The RH of the smallest active rain, P24/04/1984 (Table 3), amounts to 24.9 mm, with an average RI of 21.8 mm h^{-1} (Fig. 9).

4.3 Runoff coefficients on the 35 sites

Site-specific RCs have been calculated on the basis of the IfE equations (Eq. 1). Table 5 lists the parameters *a*, *b* and SIfC for each site, and Table 6 shows a ranking of the sites according to their total RC for the 25 rainstorms. This ranking is considered as representative of the end of the rainy season in the current rainfall regime:

Table 3 Active rainfall data 1979–2012

Rainstorm date	Total RH mm	Mean RI mm h^{-1}
P04/04/1979	75.6	53.5
P20/04/1983	53.8	30.9
P10/11/1983	57.7	19.6
P27/03/1984	67.0	53.9
P24/04/1984	24.9	21.8
P16/03/1986	61.4	55.5
P14/04/1986	56.4	24.8
P06/05/1986	58.4	53.2
P16/05/1986	100.5	73.2
P29/10/1986	103.1	62.9
P08/02/1990	82.0	40.3
P09/12/1990	41.4	25.2
P13/11/1991	56.7	24.7
P16/01/1992	104.0	30.9
P09/05/1993	55.3	9.7
P23/05/1995	59.9	42.1
P12/04/1998	118.5	81.8
P14/11/1998	46.3	12.1
P20/03/2001	55.1	31.1
P20/04/2002	57.0	18.3
P06/05/2002	97.1	63.9
P07/11/2002	40.9	6.1
P19/04/2005	33.3	65.9
P08/11/2012	20.2	15.4
P20/11/2012	62.6	15.3
Mean	63.6	–
Min	20.2	6.1
Max	118.5	81.8

Table 4 Pluviophases of three active rainstorms: 4.9, 67.0 and 118.5 mm

Rainfall date	Pluviophases		
	RH (mm)	Duration (min)	RI (mm h^{-1})
24/04/1984	1.8	30	3.6
	5	10	30.0
	5	5	60.0
	5	10	30.0
	5	75	4.0
	3.1	55	3.4
Total	24.9	185	21.8
27/03/1984	5	65	4.6
	5	5	60.0
	5	2	150.0
	5	5	60.0
	5	4	75.0
	5	6	50.0
	5	4	75.0
	5	5	60.0
	5	6	50.0
	5	5	60.0
	5	5	60.0
	5	8	37.5
	5	72	4.2
	2	15	8.0
Total	67	207	53.9
12/04/1998	3.5	5	42.0
	5	3	100.0
	5	5	60.0
	5	2	150.0
	5	5	60.0
	5	5	60.0
	5	7	42.9
	5	6	50.0
	5	11	27.3
	5	8	37.5
	5	2	150.0
	5	4	75.0
	5	2	150.0
	5	2	150.0
	5	3	100.0
	5	3	100.0
	5	5	60.0
	5	5	60.0
	5	2	150.0
	5	3	100.0
	5	3	100.0

Table 4 continued

Rainfall date	Pluviophases		
	RH (mm)	Duration (min)	RI (mm h^{-1})
	5	3	100.0
	5	10	30.0
	5	33	9.1
Total	118.5	137	81.8

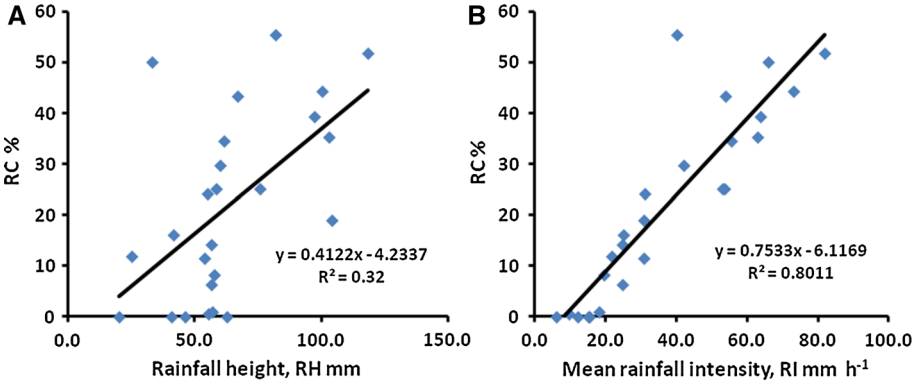

Fig. 9 Rainfall characteristics and RC. **A** Low correlation between RH (=*X*) and RC (=*Y*), **B** high correlation between RI (=*X*) and RC (=*Y*)

a. The first place is occupied by surfaces artificially over-compacted, like earthen roads, and they produce a mean RC of 96 %.
b. On the second place comes ERAIFT (RC = 40.7 %), a bare soil, with a moderate dry bulk density of 1.5 g cm^{-3}, but sealed by lichen.
c. The third place is occupied by two groups of sites. The first group is represented by a few sites of complete coverage by *Cynodon dactylon* and *Paspalum notatum* like Masikita Site. The second group contains sites with other roads like Cogelos/route.
d. The further place is subdivided into two groups. The first group shows sites with grass plot and the second one with complete coverage of *Cynodon dactylon* and *Paspalum notatum.*
e. The sixth place is again subdivided into two groups. The first group comprises a few sites with grass plot, and the second contains sites with a moderate coverage of *Cynodon dactylon* and *Paspalum notatum.*
f. The second last position is occupied by three categories of sites. The presence of cultivated plot and high grass plot could be expected here because of the vegetation (Rey et al. 2004). But to this group belongs also courtyard with very low slope gradient.
g. Finally, there are sites 4, 18, 26 and 33 (Table 1), with undefined IfE: The water reserve of 500 l available for the tests was insufficient. It concerns sites with the highest infiltration capacities of Kinshasa.

Table 6 gives also the 35 site-specific RCs for three individual active rains. It concerns the smallest active rain of 24.9 mm RH (mean RI = of 21.8 mm h^{-1}), the 'moderate' rain of 67 mm RH (mean RI = 54 mm h^{-1}) and the biggest active rain of the collection, the one of 118.5 mm RH (mean RI = 82 mm h^{-1}). It appears that the size of the rainstorm

Table 5 Parameters *a*, *b*, and SIfC in the IfE equation: $a\ \mathrm{SRI}^{-b} + \mathrm{SIfC}$

Site no.	Vegetation type or soil cover	Parameters		
		a	*b*	SIfC
1	*Boerrhavia diffusa, Digitaria longiflora*	7811.7	−0.989	28
2	Earthen road	2240.4	−1.098	0
3	*Digitaria horizontalis, Eragrostis ciliaris, Tridax procumbeus*	4,000,000	−1.949	25
4	*Digitaria horizontalis*	–	–	–
5	*Hibiscus sabdarrifa, Hibiscus acetocella*	4,000,000	−2.245	17
6	*Croton hirtus, Cyperus* sp.	8227.7	−0.792	23
7	*Hyparrhenia familiaris, Digitaria horizontalis, Pennisetum polystaschyon*	80,000,000	−1.971	45
8	*Cynodon dactylon*	58,329	−0.978	29
9	Unpaved road, bare soil	280,175	−2.088	26
10	*Paspalum notatum, Digitaria horizontalis, Mariscus aletrnifolius, Cyperus distans*	3,000,000	−1.890	30
11	*Paspalum notatum, Eleusine indica, Cynodon dactylon*	110,157	−1.254	24
12	*Panicum maximum, Eleusine indica*	750,347	−2.020	24
13	*Cynodon dactylon, Cyperus* sp.	2304.8	−0.690	24
14	*Cynodon dactylon, Panicum repens*	127,112	−1.266	25
15	*Heterotis rotundifolia, Schweinckia americana*	12,751	−1.081	20
16	*Digitaria horizontalis, Scweinckia americana*	614,053	−1.513	22
17	*Cynodon dactylon*	73,557	−1.251	28
18	*Eragrostis tremula, Croton hirtus*	–	–	–
19	*Cynodon dactylon*	39,755	−1.052	29
20	*Eleusine indica, Cynodon dactylon, Paspalum notatum*	526,234	−1.896	29
21	*Schweinckia americana*	20,000,000	−2.018	27
22	*Paspalum notatum, Eleusine indica*	849,888	−1.864	28
23	Bare soil	55,551	−1.134	25
24	*Cynodon dactylon, Digitaria horizontalis*	4496.5	−0.659	30
25	*Cynodon dactylon, Eleusine indica*	811,955	−1.891	28
26	*Eleusine indica*	–	–	–
27	*Manihot esculenta*	1748.9	−0.618	23
28	*Cynodon dactylon, Eleusine indica*	26,859	−1.217	22
29	*Urena lobata, Croton hirtus*	20,000,000	−2.003	30
30	*Digitaria horizontalis, Eragrostis tremula*	33,428	−1.089	29
31	Bare soil in inhabited land	2992.6	−0.784	39
32	*Paspalum notatum*	13,370.0	−1.051	29
33	*Cynodn dactylon, Triumfetta rhomboidea, Senna occidentalis*	–	–	–
34	Unpaved area, bare soil	3618.8	−0.912	44
35	*Eleusine indica*	7,000,000	−2.077	24

influences only slightly the ranking but to a much bigger degree the importance of the site-specific RC. This suggests that not only soil and soil cover characteristics but also rainstorm characteristics govern RC. Figure 10A, B shows respectively that RC is poorly related to RH but correlated to the mean RI.

Table 6 Runoff coefficients calculated for the 35 sites

Site no.	Site name	Total RC % for the 25 active rains	RC % for P24/04/1984 RH = 24.9 mm	RC % for P27/03/1984 RH = 67.0 mm	RC % for P12/04/1998 RH = 118.5 mm	Observations
1	Laloux/Route	96.0	76	99	98	Road
5	ERAIFT	40.7	31	59	97	Bare soil with Lichen
12	Masikita	31.0	13	44	59	Other road and Complete coverage of *paspalum*
3	Maman Mobutu/1	30.7	13	47	72	
9	Cogelos/Route	30.3	17	46.5	57	
20	Djelo Binza	29.9	18	48	57	Grass plot, complete coverage of *paspalum*
15	Bois de Ndangye	29.7	9	41	57	
17	Sanga Mamba	29.0	17	48	55	
16	Jardin du Graal	28.8	17	48	55	
28	De la Paix	28.8	9.5	42	56	
35	Ngafani	27.6	11	43	54	
25	Don Bosco	25.9	12	43.5	52	
22	Secteur Météo	25.8	11	43	51.5	
11	Wamu	25.5	12	46	51	
32	Masanga Mbila	21.7	9	40	44	
10	Maman Mobutu/3	21.5	10	41	44	
2	Laloux/Bord route	21.1	9	40	46	
13	Ngamaba	19.0	7	36.5	40	Grass plot, moderate coverage of *paspalum*
14	Lycée Tobongisa	18.3	7	34	39	
21	Mettelsat	17.6	–	31.5	40	
23	Edap/Upn	17.4	6	32	37.5	
30	Bianda/2	17.0	7	33	36	
27	Madiata	16.8	4	27	37	

Table 6 continued

Site no.	Site name	Total RC % for the 25 active rains	RC % for P24/04/1984 RH = 24.9 mm	RC % for P27/03/1984 RH = 67.0 mm	RC % for P12/04/1998 RH = 118.5 mm	Observations
29	Bianda/1	15.3	–	31	36	Cultural plot, High grass plot, courtyard with very low slope
34	Kimbanseke/Parcelle	14.4	4	20	32	
31	Mazamba	13.6	4	22	31	
6	VD Funa/1	13.3	–	28	30	
19	Kibambe	13.2	–	28	32	
24	Koweit	7.2	–	12	21	
8	Cogelos/Parcelle	5.2	–	6	20	
7	VD Funa/2	4.1	–	5	18	
26	Kingu	–	–	–	–	Undefined
18	Buadi	–	–	–	–	
33	Kimbanseke/Bord route	–	–	–	–	
4	Maman Mobutu/2	–	–		–	

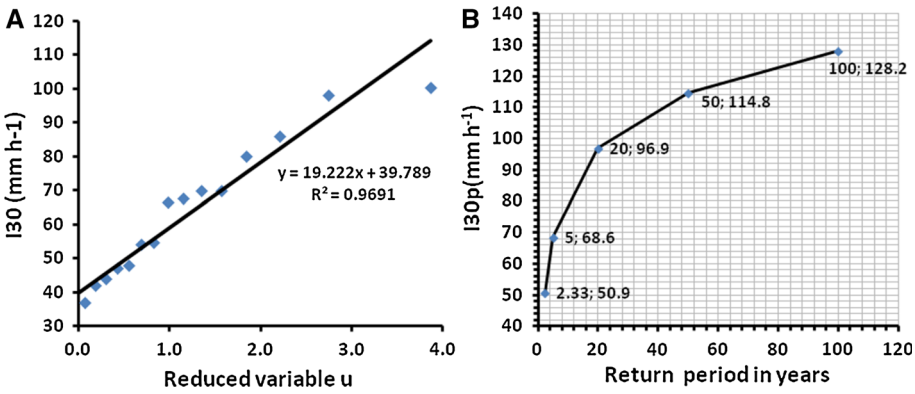

Fig. 10 **A** Frequency analysis of I30 at Kinshasa/Binza, **B** Gumbel (1958) method adjustment of I30 at Kinshasa/Binza

4.4 Critical rainstorm for sudden gully initiation or accelerated development

According to the interviews, the smallest active rain was the one of 24/04/1984 with a RH of 24.9 mm and a mean RI of 21.8 mm h^{-1} (Table 3). The rain recorded on 08/11/2012 which totals 20.9 mm RH with a mean RI of 15.8 mm h^{-1} did not provoke visible mega-gully initiation or development in the UNIKIN area and, therefore, is not considered as an active one.

Our calculations show that the smallest active rain of 24/04/1984 should provoke runoff on all tested sites, except for those with high grasses and/or those with grasses or with a bare surface but located on a slope gradient $\leq$0.08 mm^{-1}(Table 6). During the rain of 08/11/2012, apparently just below the smallest active rain, only 5 sites out of the 35 would produce runoff. It concerns Laloux/Road (RC = 86.7 %) due to its high dry bulk density of 1.9 g cm^{-3} and ERAIFT (RC = 6.1 %) because of the sealing of the surface by lichen. The other sites are Cogelos/Road (RC = 3 %) due again to the high compaction, and Djelo Binza (RC = 1.8 %) and Masikita (RC = 1.6 %) both showing a dense cover by *Cynodon dactylon* and *Paspalum notatum*.

The frequency analysis (Gumbel 1958; Beirlant et al. 2004; Reiss and Thomas 2007) of the I30 of the active rains can be used as prediction of their occurrence (Fig. 10A, B). The results show that the critical mean RI of 21.8 mm h^{-1} (Table 3) is reached every year. The maximum mean RI of 82 mm h^{-1} is reached every 11 years. The critical active rain of 24.9 mm RH occurs several times per year.

5 Discussions

5.1 Causes of inaccuracies in the site-specific RC computation

- Rainfall simulator

Possible sources of error are introduced when the rainfall simulator fails to produce during the test a constant SRI. In this case, the test has to be resumed in another impluvium with exactly the same vegetation, soil and slope gradient characteristics.

- Choice of impluvia

The intra-site variation of the site characteristics can induce various results even when the rainfall simulator works well. The choice of three impluvia showing similar characteristics is of primordial importance. In the worst case, errors are indicated by a not univoke negative relation between SRI and TR.

- Pluviophase RH

Errors can result from a subdivision of a rainstorm into pluviophases showing a too high RH. As shown in Fig. 4, TP/TR is located at the end of the pluviophase during which runoff starts. For easy computation purposes, the IfE is constructed at the right upper angle of this pluviophase. But, as a matter of fact, the IfE should start somewhere inside the pluviophase and the IfE graph should be moved more to the left. Not doing so results in an overestimation of runoff during the subsequent pluviophases. The overestimation will increase with higher pluviophase RH. Therefore, it is recommended to use rainfall records from an automatic rain gauge of the tipping bucket type, where pluviophase RH is in most cases lower than 0.5 mm.

- IfE as a proxy for IfC

It has been indicated (Sect. 3.1) that using IfE as a proxy for IfC contributes to inaccurate RC calculation. This leads possibly to a slight underestimation of RC (Fig. 7). In the case of soil uses other than road, farmland or tall and dense grass vegetation, the arbitrarily accepted SIfC (lowest SRI applied/2) leads to errors in the computation of RC that are difficult to estimate. In order to avoid this, a rainfall simulator, able to produce SRI <35 mm h^{-1}, should be used. The computation error resulting from the use of arbitrary SIfC should be less pronounced in less sandy soils where SIfC is reduced to a few mm h^{-1}. In such a case, the error in the RC computation is minimal for the common duration of natural rainfall.

5.2 Timing of field tests and validity of inter-site comparison of RC

The comparison of the site- and rainfall-specific RC of the 35 sites is based on the theoretical fact that all sites are affected at the same moment by the same rain. This implies that rainfall test and complementary soil sampling should be done on the 35 sites at the same moment, although the water content of the soil at that moment might considerably vary from site to site. However, data retrieving at one single site needs a visit of several hours, and in the best case, two sites a day could be tested. So, the testing of 35 sites took place from May 2 to August 2, 2012. This period covers the end of the rainy season and the start of the dry season and is characterized by the highest seasonally ambient soil water content.

A comparison of site-specific RCs is only possible if the RC computation concerns a same theoretical rainfall or a same series of rainfall events affecting all sites at the same time. The question arises if data input spread over the period from 2 May to 2 August allows valid inter-site RC comparison. To answer this question, all factors influencing the IfE and having a daily or seasonal evolution have to be considered. In this work, it is shown that two time-dependent factors influence the establishment of the IfE:

- The first factor is the initial water content of the upper 5 cm of the soil. Without doubt, this factor plays a role in the total infiltration capacity decay with time. But the example of site 20, Jelo Binza I and II (Fig. 7; Table 5), shows that the resulting IfE can be

nearly identical for both sites, even though inter-site as well as intra-site soil water content varies considerably.

- Secondly, there is the vegetation effect expressed by the effective infiltration surface. In sites Jelo Binza I and II, vegetation is exactly the same (Table 5). In the wet tropical climate of Kinshasa, the effective infiltration surface falls often deep below 10 %. This is the case in lawns with a root mat or in completely lichen-covered soil. In such cases, the vegetation factor, comprised in the notion of effective infiltration surface, greatly exceeds and therefore masks the capillary suction effect of the soil. In this context, it is thought that RC comparisons, based on tests during a period of decreasing change in vegetation like the period of 2 May to 2 August, are valid.

5.3 Role of vegetation in RC ranking

In many parts of the world, e.g., California (Dunne et al. 1991), Western Africa (Casenave and Valentin 1992), Queensland (Roth 2004) and Rwanda (Moeyersons 1989), increase in vegetation volume generally increases IfC: Root activity opens soil pores/fissures; the aerial part of the vegetation reduces the impact of raindrops so that formation of 'filtration pavements' (Bryan 1973) and other IfC reducing surface seals (Casenave and Valentin 1992; Poesen et al. 2003) is retarded or prevented; the aerial part of the vegetation also decreases runoff velocity, what favors IfC, or stores part of the rainfall. In Kinshasa, the porous and loose sands are not very prone to surface sealing and root activity is not needed to have high SIfC or IfC. Figure 7 shows that SIfC, derived from field rainfall simulation measurements, remains far below SIfC measured in the laboratory. In other words, the RC ranking of sites in Kinshasa results from the fact that vegetation here is lowering the IfC or SIfC instead of increasing it. This can be understood in the sense that the presence of a root mat and/or the presence of vegetation remnants lying on the ground (e.g., grass stalks and sticking leaves) increases locally the impermeability and reduces the effective soil surface through which infiltration can take place. The sealing of bare soil by lichen, mosses and algae is an extreme case of biological reduction in the effective soil surface.

The effective infiltration surface can be expressed as a percentage of the total soil surface and will mainly depend on the morphological characteristics of the vegetation at the surface of the soil and just below (e.g., root mat). In the case of farmland, hoeing temporally reduces the bulk density of the soil below natural values, what might partially or totally compensate for the reduction in effective infiltration surface. In the case of a road, the soil is artificially compacted. According to the laboratory permeameter tests, the SIfC of the soil at a dry bulk density of 1.85 g cm^{-3} should be nearly zero.

6 Conclusions and recommendations

6.1 RC ranking of representative soil uses in Kinshasa: check with current opinions—basic recommendations

The first and most striking conclusion is that both earthen and tarred roads are by far the highest runoff producers. The total RC of the earthen Laloux Road (Site 2) amounts to 96 % as calculated for 25 active rains. This explains why road control is a good proxy for the topographical control of mega-gullies in Kinshasa (Makanzu Imwangana et al. 2014a). In the high town of Kinshasa, the road network, both earthen and tarred, occupies ~13 %

of the total surface of the contributing areas to mega-gully heads and, therefore, explains a RC of ~12.5 % for the entire urban area. A densification of the road network will increase the RC. This implies that critical rain for gullying becomes a relative notion. For the actual situation in the high town of Kinshasa, the critical RH is 24.9 mm (Sect. 3.4), but this value will lower with increasing road surface percentage. One way to reduce the disastrous runoff production by roads is to develop road coatings which allow easy water infiltration. This solution aims to reduce runoff peak discharge upon and along the roads and might be an alternative for the installation of runoff diverters along the streets (Makanzu Imwangana et al. 2014a).

The second biggest RC is given by sandy soil covered by a thin layer of lichen (Site 5 ERAIFT). This confirms the ability of microorganisms, like it has also been observed in Belgium and Israel (De Ploey 1977; Yair 2006), to seal an otherwise permeable soil. Table 6 shows that RC of ERAIFT approaches RC of Laloux road for the RH of 118.5 mm. In the perspective of gully development due to Horton runoff, gullies in the high town of Kinshasa have the highest chances to develop along roads and in places where road runoff leaves the road. Also areas on bare sand with lichen should be prone to gully formation.

In the other sites, RC is considerably lower (Table 6). In the third group, RC falls below one-third of the one of Laloux road. It is interesting to see that this group includes bare surfaces together with well-developed grass plots (*Paspalum notatum* sp., *Cynodon dactylon* sp.). It concerns grass courts where the grass is regularly cut. Lawn is a type of soil use, often advised to be applied within the courtyards to reduce runoff, but this study shows that grass courts along houses are not a good solution for the runoff problem. Our observations show, indeed, that grass courts, regularly cut, not only quickly cover nearly 100 % of the soil, but develop in the same time a strong and less permeable continuous root mat.

The other sites produce a still lower RC, depending on the percentage of soil cover as well as slope gradient. A point to be raised here is that courtyards with bare soil appear only from the third group on but that they are especially present in the fifth group. This is worth of noting because Van Caillie (1983) warned for the big quantities of runoff they produce. Courtyards with a lower slope gradient, therefore, do not produce much runoff regardless of the soil use. Inhabitants should be urged to give special attention to this aspect of their courtyards. Instead of making them unsafe for children by digging deep collector holes, a very slight counter-slope of <0.08 m m^{-1} should allow quasi-complete infiltration of rain water in most of the cases. Of course roof water can cause a problem in the compound if not collected, e.g., in a sink pit.

6.2 Early warning system for gullying and global change effects

The critical (RH-RI) combination for gulling in Kinshasa can be used by the meteorological services of DR Congo to add early warnings to the weather forecast.

Table 6 illustrates that RC not only is a function of soil use, soil compaction and slope gradient but also of the simple rainstorm parameters RH and RI. This indicates that changes in pluviometric regime can induce changes in the feeding of gullies and in the hydrological cycle in general. The trend, indicated in Table 6, is such that a regime with higher and more intense rainfall (Fig. 9B) will create higher RCs, especially in sites which today display a comparative low RC. Ntombi et al. (2009), on the basis of pluviometric analysis of data from the period of 1991–2005, think that in the future heavy and big rains

will become more frequent. This should be a starting point for initiating research into that direction to provide solutions for adaptation strategies.

6.3 Calibration of the new method of RC assessment

The inaccuracies presented in Sect. 5.1 show that the proposed method of RC assessment is still in the experimental phase. The use of IfE as a proxy for Horton IfC leads to a small RC underestimation, which might be partially compensated for by overestimation due to high pluviophase RH. Other inaccuracies stem from inadequate choice of intra-site test impluvia and from material defects. Although the method is basically sound and the results are logical, a comparison with data from field stations could lead to still more accurate RC assessment.

Acknowledgments The authors thank the Frame Agreement between Belgium and the DR Congo concerning the Institutional Collaboration between the Royal Museum for Central Africa (Tervuren, Belgium) and the 'Centre de Recherches Géologiques et Minières' (Kinshasa, DR Congo).

References

Arnaez J, Larrea V, Ortigosa L (2004) Surface runoff and soil erosion on unpaved forest roads from rainfall simulation tests in northeastern Spain. Catena 57:1–14

Beirlant J, Goegebeur Y, Segers J, Teugels J (2004) Statistics of extremes: theory and applications. Wiley, London

Ben-Asher J, Humborg G (1992) A partial contributing area model for linking rainfall simulation data with hydrographs of a small arid watershed. Water Resour Res 28:2041–2047

Bryan RB (1973) Surface trusts formed under simulated rainfall on Canadian soils. Report to a conference held in Pisa, CNR, 30p

Bultot F (1971) Statistiques des pluies intensives en un point dans une aire du Congo belge et du Ruanda – Urundi. B.C.C.V, 11, Bruxelles, 136p

Cahen L (1954) Géologie du Congo belge. H. Vaillant-Carmanne, Liège

Casenave A, Valentin C (1992) A runoff capability classification system based on surface features criteria in semi-arid areas of West Africa. J Hydrol 130(23):1–249

Darcy H (1856) Les fontaines publiques de la ville de Dijon. Dalmont, Paris

De Maximy R (1978) Site général de Kinshasa. In: Atlas de Kinshasa, Planche 1, B.E.A.U/T.P.A.T, IGN – Paris

De Maximy R, Van Caillie X (1978) Géomorphologie de Kinshasa. In: Atlas de Kinshasa, Planche 8, B.E.A.U/T.P.A.T, IGN – Paris

De Ploey J (1963) Quelques indices sur l'évolution morphologique et paléoclimatique des environs du Stanley-Pool (Congo). Faculté des Sciences, Studia Universitatis «Lovanium» 17, Ed. de l'Université, Léopoldville, 16 p+Annexes

De Ploey J (1977) Some experimental data on slopewash and wind action with reference to quaternary morphologenesis in Belgium. Earth Surf Process Land 2:101–115

Dewitte O, Daoudi M, Bosco C, Van Den Eeckhaut M (2015) Predicting the susceptibility to gully initiation in data-poor regions. Geomorphology 228:101–115

Duiker SW, Flanagan DC, Lal R (2001) Erodibility and infiltration characteristics of five major soils of southwest Spain. Catena 45:103–121

Dunne T, Zhang W, Aubry BF (1991) Effects of rainfall, vegetation, and microtopography on infiltration and runoff. Water Resour Res 27(9):2271–2285

Egoroff A (1955) Esquisse géologique provisoire du sous-sol de Léopoldville. Service géologique du Congo belge et du Ruanda-Urundi, 6, 15p

Esteves M, Planchon O, Lapetite JM, Silvera N, Cadet P (2000) The «EMIRE» large rainfall simulator: design and field testing. Earth Surf Process Land 25:681–690

Ferreira CSS, Ferreira AJD, Pato RL, Do Carmo Magalhaes M, De Olivera Coelho C, Santos C (2012) Rainfall–runoff–erosion relationships study for different land uses, in a sub-urban area. Zeitschrift für Geomorphologie 56:005–020

Garcia-Ruiz JM (2010) The effects of land uses on soil erosion in Spain. A review. Catena 81:1–11
Graf WL (1977) The rate law in fluvial geomorphology. Am J Sci 277:178–191
Gumbel EJ (1958) Statistics of extremes. Columbia University Press, New York
Hamed Y, Albergel J, Pépin Y, Asseline J, NaIs S, Zante P, Berndtsson R, El-Niazy M, Balah M (2002) Comparison between rainfall simulator erosion and observed reservoir sedimentation in an erosion-sensitive semiarid catchment. Catena 50:1–16
Horton RE (1933) The role of infiltration in the hydrologic cycle. Trans Am Geophys Union 14:446–460
Horton RE (1945) Erosional development of streams and their drainage basins: hydrophysical approach to quantitative morphology. Bull Geol Soc Am 56:275–330
Hôtel de Ville de Kinshasa (2007) Programme du gouvernement provincial de Kinshasa 2007–2011, HVK, inédit, 94p
Hudson NW (1971) Soil conservation. Batsford, London
Kikufi BA, Lukoki FL (2008) Etude floristique et écologique des marais de Masina. Revue Congolaise des Sciences Nucléaires 23:1–20
Lambe TW, Whitman RV (1979) Soil mechanics, S.I. Version. Wiley, New York
Lasanta T, Garcia-Ruiz JM, Pérez-Rontonné C, Sancho Marcén C (2000) Runoff and sediment yield in a semi-arid environment: the effect of land management after farmland abandonment. Catena 38:265–278
Laws JO (1941) Measurement of the fall velocity of waterdrops and raindrops. Trans Am Geophys Union 22:709
Li XY, Contreras S, Solé-Benet A, Canton Y, Domingo Fr, Lazaro R, Lin H, Van Wesemael B, Puigde-fabregas J (2011) Controls of infiltration–runoff processes in Mediterranean karst rangelands in SE, Spain. Catena 86:98–109
Makanzu Imwangana F (2010) Etude de l'érosion ravinante à Kinshasa par télédétection et SIG entre 1957 et 2007. Advanced master thesis, Faculty of Sciences, DSGE/ULg, 76p
Makanzu Imwangana F, Ozer P, Moeyersons J, Vandecasteele I, Trefois P, Ntombi M (2012) Kinshasa en proie à l'érosion en ravine: inventaire et impact socio-économique."Colloque international sur le thème : Géomatique et gestion des risques naturels en hommage au Professeur André OZER'', 6–8 mars 2012, UMP, Oujda, Maroc. Volume de résumés, p 27
Makanzu Imwangana F, Moeyersons J, Ntombi M (2013) Factors in the development of urban mega-gullies in the high town of Kinshasa. In: 6th ISGE, IASI/Romania, Book of abstracts, p 27
Makanzu Imwangana F, Dewitte O, Ntombi M, Moeyersons J (2014a) Topographic and road control of mega-gullies in Kinshasa (DR. Congo). Geomorphology 217:131–139
Makanzu Imwangana F, Vandecasteele I, Ozer P, Trefois P, Moeyersons J (2014b) The origin and control of mega-gullies in Kinshasa (DR Congo). Catena 125:38–49
Martinez-Murillo JF, Nadal-Romero E, Regués D, Cerdà A, Poesen J (2013) Soil erosion and hydrology of the western Mediterranean badlands throughout rainfall simulation experiments: a review. Catena 106:101–112
Moeyersons J (1978) The behaviour of stones and stone implements buried in consolidating and creeping Kalahari sands. Earth Surf Process Land 3:115–128
Moeyersons J (1989) La nature de l'érosion des versants au Rwanda. Annales des Sciences économiques, Musée royal de l'Afrique centrale (MRAC), Tervuren, Belgique, 19, 379p
Nadal-Romero E, Lansanta T, Garcia-Ruiz JM (2013) Runoff and sediment yield from land under various uses in a Mediterranean mountain area: long-term results from an experimental station. Earth Surf Proc Land 38:346–355
Ntombi MK, Yina N, Kisangala M, Makanzu IMF (2004) Evolution des précipitations supérieures ou égales à 15 mm durant la période 1972–2002 à Kinshasa. Revue Congolaise des Sciences Nucléaires 20:30–40
Ntombi MK, Pangu S, Mukunayi N, Kisangala M, Ntombi MM, Makanzu F (2009) Les ressources en eau et les changements climatiques en cours en République Démocratique du Congo. In: Endundo José, "Seconde communication nationale à la Convention Cadre sur le Changement Climatique." Ministre de l'Environnement, Conservation de la Nature et Tourisme de la RD.Congo. Kinshasa, november 2009. Présentée à la Communauté internationale en réponse au Protocole de KYOTO
Pain M (1984) Kinshasa – la ville et la cité, études urbaines. ORSTOM/Paris, Mémoires 105, 267p
Peel MC, Finlayson BL, McMahon TA (2007) Updated World map of the Köppen–Geiger climate. Hydrol Earth Syst Sci 11:1633–1644
Poesen J, Nachtergaele J, Verstraeten G, Valentin C (2003) Gully erosion and environmental change: importance and research needs. Catena 50:91–133
Poulenard J, Podwojewski P, Janeau JL, Collinet (2001) Runoff and soil erosion under rainfall simulation of Andisols from the Ecuadorian Paramo: effect of tillage and burning. Catena 45:185–207

Prosser IP, Dietrich WE (1995) Field experiments on erosion by overland flow and their implication for a digital terrain model of channel initiation. Water Resour Res 31(11):2867–2876

Prosser IP, Slade CJ (1994) Gully formation and the role of valley-floor vegetation, southeastern Australia. Geology 22:1127–1130

Reiss R-D, Thomas M (2007) Statistical analysis of extreme values, with application to insurance, finance, hydrology and other fields, vol 18, 3rd edn. Birkhäuser, Basel

Rey F, Ballais J-L, Marre A, Rovéra G (2004) Rôle de la végétation dans la protection contre l'érosion hydrique de surface. Comptes Rendus Geosci 336:991–998

Römkens MJM, Helming K, Prasad SN (2001) Soil erosion under different rainfall intensities, surface roughness, and soil water regimes. Catena 46:103–203

Roth CH (2004) A framework relating soil surface condition to infiltration and sediment and nutrient mobilization in grazed rangelands of northeastern Queensland, Australia. Earth Surf Process Landf 29:1093–1104

Smith RE (1972) The infiltration envelope: results from a theoretical infiltrometer. J Hydrol 17:1–21

Tshibangu KWT, Engels P, Malaisse F (1997) Evolution du couvert végétal dans la région de Kinshasa (1960–1987) selon une approche cartographique. Geo-Eco-Trop 21:95–103

Van Caillie X (1983) Hydrologie et érosion dans la région de Kinshasa : Analyse des interactions entre les conditions du milieu, les érosions et le bilan hydrologique. Thèse de doctorat, Dpt de Geografie Geologie, KUL, 554p

Yair A (2006) Runoff generation in a sandy area-the nizzana sands, Western Negev, Israel. Earth Surf Process Land 15:597–609